

# Impact of Rebar-Reinforcement on Flexural Response of Shear-Critical Ultrahigh-Performance Concrete Beams

Yassir M. Abbas, Mohammad Iqbal Khan, Galal Fares

**Abstract**—In the present work, the structural responses of 12 ultra-high-performance concrete (UHPC) beams to four-point loading conditions were experimentally and analytically studied. The inclusion of a fibrous system in the UHPC material increased its compressive and flexural strengths by 31.5% and 237.8%, respectively. Based on the analysis of the load-deflection curves of UHPC beams, it was found that UHPC beams with a low reinforcement ratio are prone to sudden brittle failure. This failure behavior was changed, however, to a ductile one in beams with medium to high ratios. The implication is that improving UHPC beam tensile reinforcement could result in a higher level of safety. More reinforcement bars also enabled the load-deflection behavior to be improved, particularly after yielding.

**Keywords**—Ultra-high-performance concrete, moment capacity, RC beams, hybrid fiber, ductility.

## I. INTRODUCTION

UHPC is a relatively novel fibrous cementitious composite. It is characterized by its ultra-high compressive strength, low water to cement content (usually less than 25%), superior packing density, impact resistance, flowability, and long-lasting characteristics [1]-[3]. The generally acknowledged minimum compressive strength level of UHPC is 150 MPa. However, it is practical to allow for the broader domain of UHPC's strengths, as investigators employ various standardized methods for strength assessment [4]. The compact microstructure of UHPC is obtained by optimizing its packing density. The latter significantly affects the compressive strength and waterproofness (i.e., enhances the permanency features) [2]. UHPC normally incorporates steel fibers to enhance its ductility response to tensile forces [5]. The technology for developing UHPC involves properly mixing Portland and other types of cement with an optimized aggregate size distribution, fibrous reinforcement, and employment of chemical admixtures (superplasticizers).

The guidelines for designing normal concrete structures have been successfully developed by many building codes such as ACI (American Concrete Institute), IBC (International Building Code), Eurocode, etc., which have been utilized in design practice for many years [6]. Nevertheless, these guidelines do not apply for recently developed UHPC structural members, since its intrinsic mechanical properties (i.e., tensile, compressive, and fracture energy) are quite different from normal concrete. It is noteworthy that some references on the

prediction of the ultimate moment of UHPC structural elements are available in [7]-[9]; however, these methods have not yet been adopted in the international design codes, as far as we are concerned. Additionally, many prediction formulas have been developed that incorporate the inelastic response of UHPC [10]-[15]. These references have been fundamentally employed in the moment-curvature prediction. It involves the utilization of the tensile and compressive constitutive stress-strain models with experimental investigations, which are problematic for design purposes. For these purposes, the establishment of simplified prediction models for the ultimate moment is therefore of great importance. Significant research efforts have been devoted to structural elements developed by high- and ultra-high-performance reinforced concrete. Such studies are conducted to investigate the sectional stress and strain distributions, the physicomechanical characteristics (i.e., tensile strength, shape, aspect ratio, etc.), and content, dispersion, the bonding strength of fibers, and other factors impacting the tensile behavior of UHPC [15]-[23]. However, these investigations have only addressed the use of single-kind fibers, and very little information (e.g., [6]) is obtainable on the use of a hybrid system of fibers in UHPC.

In the current research, the primary goal was to study the structural performance of shear-deficient UHPC hybrid fiber-reinforced beams and to develop a reliable prediction model for their ultimate moment strength. Thus, 12 beams with various longitudinal bar arrangements were developed with low-to-high reinforcement percentages (0%, 0.54%, 0.84%, 1.21%, 2.14%, and 3.35%). All beams were prepared using a UHPC mixture containing 2.58% (vol.) of a hybrid system of smooth-coated fibers with various lengths and a unified diameter (0.2 mm), and tested under four-point loading conditions. In this work, the observed structural response (load-deflection and moment-curvature curves, ductility, crack response, and failure patterns) of beams is presented and discussed.

## II. EXPERIMENTAL PROGRAM

### A. Materials

Ordinary Portland cement (PC) complying with ASTM C150 specifications was used as the main constituent for the binder formulated with silica fume (SF) and class F fly ash (FA) as supplementary cementitious materials. Table I lists the physicochemical properties of the employed types of cement.

Yassir M. Abbas\*, Mohammad Iqbal Khan, and Galal Fares are with Department of Civil Engineering, College of Engineering, King Saud

University, Riyadh 800-11421, Saudi Arabia (\*corresponding author, e-mail: yabbas@ksu.edu.sa).

The specific gravities of PC, SF, and FA were 3.15, 2.2, and 2.7, respectively. Furthermore, Arabian Peninsula-based sands (characterized as red dune (RS) and white (WS)) were employed as fine aggregates. The specific gravities of RS and WS at saturated surface dry conditions (SSD) were 2.65 and 2.74, respectively. An Axios Max X-ray fluorescence (XRF) machine was utilized to determine the chemical composition of the binder constituting powders. The particle-size distribution (PSD) analysis of the fine powders was conducted using a laser diffraction particle size analyzer (LA-950). Microstructural analysis was conducted employing a Versa 3D dual beam field emission scanning electron microscope (SEM). Fig. 1 (a) depicts the grain size distribution curves for PC, FA, and SF, whereas Fig. 1 (b) and Table II illustrate the PSD analysis and physical properties of the employed aggregates.

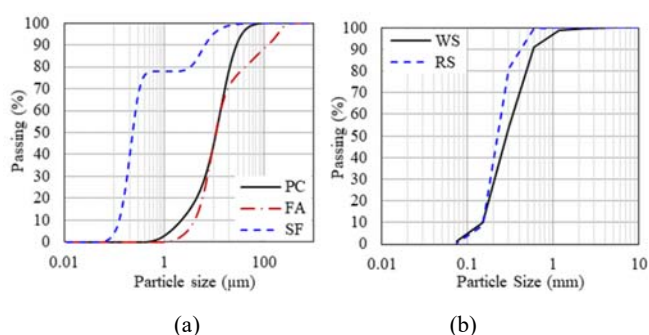


Fig. 1 Grain size distribution of (a) types of cement and (b) aggregates

TABLE I  
PHYSICOCHEMICAL PROPERTIES OF PC AND SCMS

Oxides (%)	PC	FA	SF
SiO <sub>2</sub>	20.41	55.23	86.20
Al <sub>2</sub> O <sub>3</sub>	5.32	25.95	0.49
Fe <sub>2</sub> O <sub>3</sub>	4.10	10.17	3.79
CaO	64.14	1.32	2.19
MgO	0.71	0.31	1.31
SO <sub>3</sub>	2.44	0.18	0.74
TiO <sub>2</sub>	0.30	-	-
Na <sub>2</sub> Oeq	0.10	0.86	2.80
L.O.I.	2.18	5.00	2.48
Relative density	3.15	2.70	2.20

TABLE II  
PHYSICAL PROPERTIES OF RS AND WS

Property	RS	WS
Bulk specific gravity (OD basis)	2.64	2.73
Apparent specific gravity	2.67	2.76
Absorption, %	0.30	0.37
Fineness modulus (range of 2.3–3.1)	1.11	1.46

In this experimental investigation, a hybrid system of three fibers (designated as A, B, and C) bright high-carbon and high-performance strength microsteel straight fibers were used as discontinuous reinforcement of the developed UHPC mixes. The physical and mechanical properties (as received) of the microsteel fibers are given in Table III. The mix design of the UHPC is detailed in Table IV. It is worth noting that a

polycarboxylate ether-based water reducer superplasticizer [commercially recognized as Master Glenium 51 (Master Builders Solutions UK Ltd, Manchester, UK)] was identified as SP and employed in the current study to control the workability of the pre-prepared mixes. This SP had a density and water content of 1080 kg/m<sup>3</sup> and 65.19%, respectively. To this end, the quantity of water contained in the SP was corrected in the calculation of the amount of mixing water after the water-to-binder ratio was optimized as 0.165.

TABLE III  
PHYSICOMECHANICAL PROPERTIES OF FIBERS

Fiber	Length (mm)	Diameter (μm)	Tensile Strength (MPa)
A	13		
B	20	200	2600
C	30		

TABLE IV  
MIX DESIGN OF THE UHPC (IN KG/M<sup>3</sup>)

PC	SF	FA	WS	RS	Water	SP	Fiber		
							A	B	C
1123	239	66	481	161	213	40	152	43	8

### B. Methods

In the current study, the UHPC was prepared using a dissolver mixer [MischTechnik, UEZ ZZ 50-S with 95 L capacity (UEZ Mischtechnik GmbH, Stuttgart, Germany)]. Firstly, all the dry materials (PC, FA, SF, WS, and RS) were mixed for 5 min at high rotation speed (about 743 rpm) to achieve their highest analogy. Secondly, the mixing water, which was blended with SP, and the aggregates' absorption water were added during mixing for 10 min until the flowability of the mix was in the range of 180–220 mm. The flowability was measured following the ASTM C 1437. Afterward, the weighed hybrid system of fibers was gradually poured into the wet mix in slight dosages for ideal diffusion at a slow rotation pace (about 371 rpm) for 2 min. After the addition of fibers, the mixing speed was converted to intermediate. This last stage of mixing took 3–8 min to develop satisfactory homogenization of the UHPC. Eventually, the produced UHPC was poured (in 50 mm layers) into the beam' molds, which included the pre-placed steel bars. To investigate the compressive and flexural strength of the UHPC, 50 mm cubes and (75 mm × 75 mm × 300 mm) prism samples were additionally prepared. All UHPC specimens were cured for 28 days under standard saturated curing conditions (21 ± 2 °C temperature and 100% relative humidity).

In this study, 12 mini-scale UHPC rectangular beams were prepared for the experimental investigation. The size of beam test specimens was 150 mm × 150 mm × 600 mm. Fig. 2 shows the geometry and reinforcement properties. It is noteworthy that the bottom and side cover of bars were 20 mm. Moreover, a set of prefabricated concrete spacers (20 × 20 × 20 mm) was used to fix the single-layer reinforcing bars. Table V lists the details of the beam's bars and their percentages of reinforcement. In the current investigation, the key variable between the various beam sets was the percentage of the tensile reinforcement.

The compressive strength of the UHPC samples was

determined using a universal compression testing machine (Instron (Norwood, Massachusetts, US), with a capacity of 3000 kN). This test was accomplished in compliance with ASTM C109 specifications of a constant loading rate of 0.2 MPa/s. It is worth noting that previous studies on the compressive behavior of UHPC using the ASTM C109 standard and cubic specimens have shown closely comparable results to the response obtained by the ASTM C39 by employing cylindrical specimens. Accordingly, the cubic concrete samples that do not require preparation of their ends have the potential to effectively substitute for the cylindrical ones [24].

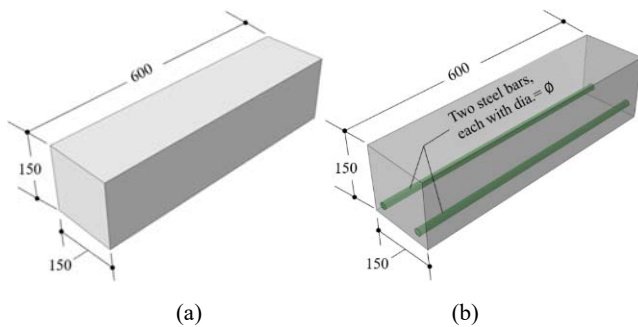


Fig. 2 The details of (a) B1 and (b) B2–B6 (Dimensions are in mm)

TABLE V  
REINFORCEMENT DETAILS FOR BEAM SPECIMENS

No.	Code	$\phi$ (mm)	Reinforcement Ratio, $\rho$ (%)
1	B1	-	-
2	B1-R	-	-
3	B2	8	0.54
4	B2-R	8	0.54
5	B3	10	0.84
6	B3-R	10	0.84
7	B4	12	1.21
8	B-R	12	1.21
9	B5	16	2.14
10	B5-R	16	2.14
11	B6	20	3.35
12	B6-R	20	3.35

The flexural test was conducted according to ASTM C1609. Beneath the sample, two linear variable differential transformers (LVDTs, Tokyo Sokki, model FDP 50A with  $300 \times 10^{-6}$  strain/mm sensitivity (Tokyo, Japan)) were installed to measure the mid-span displacement of the samples during the test. Moreover, a 30 kN universal testing machine (INSTRON, Model 3367 (Norwood, Massachusetts, US)) was employed to conduct the flexural test at a loading rate of 0.2 mm/min. It worth noting that the two LVDTs were connected to a data acquisition system (Tokyo Sokki, model TDS-630 with a speed of 1000 channels in 0.1 s) to synchronize and acquire the test data. The compressive and flexural tests were conducted on UHPC samples with and without fibers (UHPC-C) for comparison purposes.

In the current research, the mechanical properties of the steel bars were evaluated by performing the uniaxial tensile test using 600 mm (length) specimens as per ASTM A370

specifications. The test was conducted under displacement-controlled conditions at a rate of 0.0187 mm/s. From this test, the stress–strain behavior of the high-strength steel was obtained and utilized to evaluate the material’s yield strength and Young’s modulus. It is worth noting that the result for the earlier material tests represents the average of three samples.

In the current investigation, the structural behavior of the control and reinforced UHPC beams (Fig. 2 and Table V) was investigated under four-point loading conditions. The test’s schematic diagram is shown in Fig. 3. This test was performed by utilizing Toni Technik’s servo-controlled hydraulic universal testing machine (Model 2073, 3000-kN capacity). The instrumentation during the test included three strain gauges attached to the specimen’s top and front faces to measure the strain response of concrete. Two strain gauges were additionally attached to the embedded reinforcement of B2–B6 in order to acquire the tensile strain of steel bars.

Moreover, two linear variable differential transformers (LVDTs—Tokyo Sokki, model FDP 50A with  $300 \times 10^{-6}$  strain/mm sensitivity) were attached at the specimen’s mid-span to obtain its real-time mean deflection. Moreover, two horizontal/inclined LVDTs were fixed to measure the crack width after its initiation. In the current experimental testing, displacement-controlled loading conditions were applied at a rate of 0.4 mm/min to the beam’s top surface (Fig. 4 (a)) until final failure. It is worth mentioning that all the earlier-described accessories (LVDTs, strain gauges, and load cell) were synchronized to a data acquisition system (Tokyo Sokki, model TDS-630 with a speed of 1000 channels in 0.1 s) to gain the test data. Additionally, high-resolution photographs were taken for the 12 beams after the accomplishment of each test to assess their failure pattern.

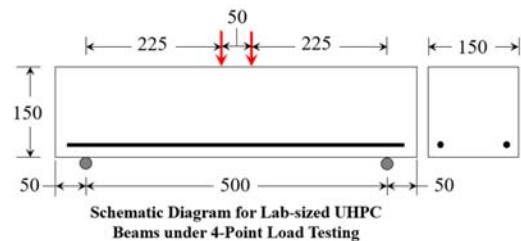


Fig. 3 Testing of beams under four-point loading.

### III. RESULTS AND DISCUSSION

#### A. Material Properties

The observed average 28-day compressive strength of UHPC mixes (Table IV) with and without fibers (UHPC-C) under normal curing conditions were 143 and 188 MPa, respectively. Further, the mean flexural strengths for UHPC-C and UHPC were 4.3 MPa and 15.2 MPa, respectively. Additionally, the uniaxial testing of steel bars showed that the ultimate yield strength and Young’s modulus of the employed steel bars for longitudinal reinforcement of beams were 520 MPa and 210 GPa, respectively.

### B. Flexural Behavior of Beams

The load–deflection responses of B1–B6 and their replicas are presented in Fig. 4, obtained from the four-point loading test. For all beams, this figure demonstrated that repeatability of acceptable results has been accomplished, as close curves were obtained for the duplicated specimens. Fig. 4 demonstrated that increasing the amount of tensile reinforcement in the UHPC beams could increase the load-bearing capacity and change the failure pattern from brittle to ductile. In this context, B6 (Fig. 4 (f)) represents a typical reinforced concrete beam behavior. According to this finding, fibers are likely of marginal importance in accelerating the load-bearing of shear-deficient UHPC beams.

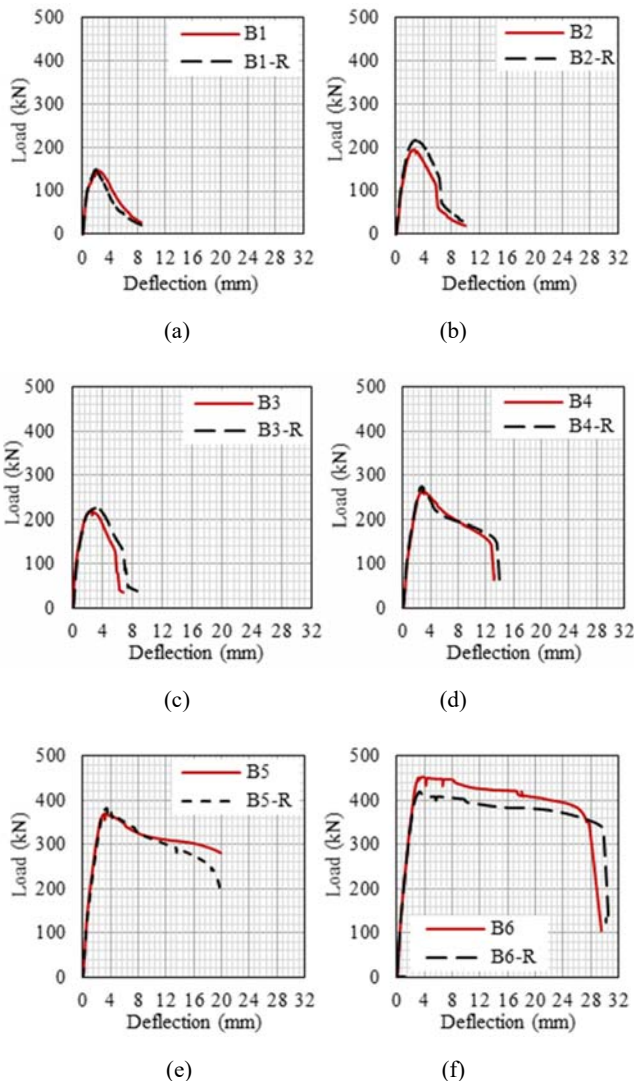


Fig. 4 Load–deflection responses of: (a) B1, (b) B2, (c) B3, (d) B4, (e) B5, and (f) B6

Fig. 5 (a) displays a comparison of the representative load–deflection curves for the tested UHPC beams. As expected, for the beams with low reinforcement percentages (0–0.84% (B1–B3)), a sudden brittle flexural failure was observed. However, the use of the medium to high  $\rho$  (1.21–3.35% (B4–B6)) altered

this failure behavior to semi-ductile to ductile ones. Fig. 5 (a) also shows the loading and energy absorption capacities (especially after yielding the bar reinforcement), as would be anticipated. Moreover, the ultimate midspan deflection of the UHPC beams with low reinforcement percentages (B1–B3) was almost constant (about 8 mm) and increased as their reinforcing content increased; however, it notably increased as it reached higher reinforcement levels (B4 to B6). This displacement response could be attributed to the brittle behavior of the first three beams (failure occurred right after the ultimate loading) compared to the improved deformability of the latter beams. Fig. 5 (b) shows the relation between the beam’s ultimate load and reinforcement ratio. The trend of this relation was fairly linear, with a 96% confidence level (coefficient of correlation).

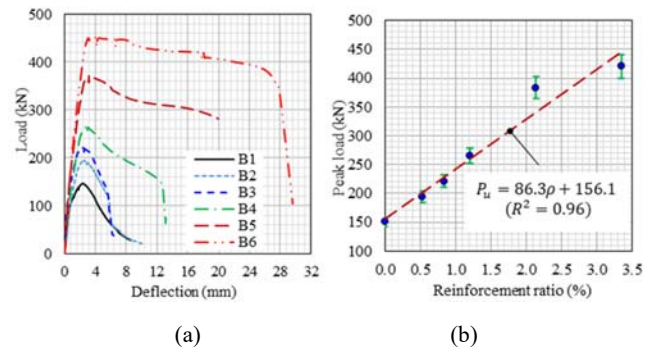


Fig. 5 Load–deflection of beams and (b) peak load-reinforcement ratio relation

### IV. CONCLUSIONS

The intertwining of the three types of fibers has enabled an enhanced pullout mechanism in a cementitious matrix with low water content. Based on the fact that fibers with shorter aspects become more numerous than longer fibers under the same proportion, shorter microfibers are more likely to be unidirectional and compactly distributed in the axial axis of the highly compacted and flowable cementitious matrix under the concrete pouring direction. Accordingly, short microfibers become more effective in controlling the initiation and propagation of microcracks while the longer fibers control the macrocracks. As a result, this ternary combination would prevent micro- and macro-crack growth in the generated cementitious matrix. The concept of high packing density and highly distributed microfibers due to the selected additives with optimal proportions is validated through the performance-based approach relied on post-cracking strength and toughness. In the current research, the experimental mechanical response to the four-point loading condition of UHPC beams was accordingly discussed. Based on this study, the following conclusions were drawn:

- The inclusion of the fibrous system of fibers in the UHPC concrete increased its compressive and flexural strengths by 31.5% and 237.8%, which indicated the significance of fibers in promoting the tensile and flexural properties of UHPC.
- The investigation of the load–deflection curves of beams

revealed that the UHPC beams with low  $\rho$  failed by a sudden brittle flexural failure; however, the beams with medium to high  $\rho$  altered this failure behavior to semi-ductile to ductile ones. This conclusion implies that better safety could be achieved by optimizing the tensile reinforcement for a UHPC beam. Additionally, the entire load–deflection behavior was enhanced by the introduction of more bar reinforcement (especially after yielding the bar reinforcement).

#### DECLARATION OF CONFLICT OF INTERESTS

We declare that there is no conflict of interest. They have no known competing financial interests or personal relationships that could have appeared to influence the work reported in this paper.

#### REFERENCES

- [1] Naaman AE, Wille K. The path to ultra-high performance fiber reinforced concrete (UHP-FRC): five decades of progress. *Proceedings of Hipermat*. 2012;3-15
- [2] Manglekar HC, Visage ET, Ray T, Weldon BD. Experimental and Analytical Investigations of a Locally Developed Ultrahigh-Performance Fiber-Reinforced Concrete. *J Mater Civ Eng*. 2017;29:10.10.1061/(asce)mt.1943-5533.0001732
- [3] Yoo D. Performance enhancement of ultra-high-performance fiber-reinforced concrete and model development for practical utilization. Seoul: Korea University. 2014
- [4] Naaman AE. Half a century of progress leading to ultra-high performance fiber reinforced concrete: part 1-overall review. *Proceedings of the 2nd International RILEM Conference2011*. p. 17-26.
- [5] Baby F, Marchand P, Toutlemonde F. Shear Behavior of Ultrahigh Performance Fiber-Reinforced Concrete Beams. I: Experimental Investigation. *J Struct Eng*. 2014;140:10.10.1061/(asce)st.1943-541x.0000907
- [6] Turker K, Hasgul U, Birol T, Yavas A, Yazici H. Hybrid fiber use on flexural behavior of ultra high performance fiber reinforced concrete beams. *Composite structures*. 2019;229:111400
- [7] Yokota H, Rokugo K, Sakata N. *JSCCE recommendations for design and construction of high performance fiber reinforced cement composite with multiple fine cracks. High Performance Fiber Reinforced Cement Composites*; Springer: Tokyo, Japan. 2008
- [8] Fehling E, Schmidt M, Walraven J, Leutbecher T, Fröhlich S. *Ultra-high performance concrete UHPC: Fundamentals, design, examples*: John Wiley & Sons; 2015.
- [9] Graybeal BA. *Material property characterization of ultra-high performance concrete*. United States. Federal Highway Administration. Office of Infrastructure ...; 2006.
- [10] Yang IH, Joh C, Kim B-S. Structural behavior of ultra high performance concrete beams subjected to bending. *Engineering Structures*. 2010;32:3478-87.<http://dx.doi.org/10.1016/j.engstruct.2010.07.017>
- [11] Yoo D-Y, Yoon Y-S. Structural performance of ultra-high-performance concrete beams with different steel fibers. *Engineering Structures*. 2015;102:409-23.<https://doi.org/10.1016/j.engstruct.2015.08.029>
- [12] Yoo D-Y, Banthia N, Yoon Y-S. Experimental and numerical study on flexural behavior of UHPFRC beams with low reinforcement ratios. 2017.<http://www.nrcresearchpress.com/doi/abs/10.1139/cjee-2015-0384>
- [13] Singh M, Sheikh AH, Mohamed Ali MS, Visintin P, Griffith MC. Experimental and numerical study of the flexural behaviour of ultra-high performance fibre reinforced concrete beams. *Construction and Building Materials*. 2017;138:12-25.10.1016/j.conbuildmat.2017.02.002
- [14] Yang I-H, Joh C, Kim B-S. Flexural response predictions for ultra-high-performance fibre-reinforced concrete beams. *Mag Concr Res*. 2012;64:113-27.<https://doi.org/10.1680/macrc.10.00115>
- [15] Xia J, Chan T, Mackie KR, Saleem MA, Mirmiran A. Sectional analysis for design of ultra-high performance fiber reinforced concrete beams with passive reinforcement. *Engineering Structures*. 2018;160:121-32.<https://doi.org/10.1016/j.engstruct.2018.01.035>
- [16] Dancygier A, Savir Z. Flexural behavior of HSFRC with low reinforcement ratios. *Engineering structures*. 2006;28:1503-12
- [17] Yang I-H, Joh C, Kim B-S. Flexural strength of large-scale ultra high performance concrete prestressed T-beams. *Canadian Journal of Civil Engineering*. 2011;38:1185-95.<https://doi.org/10.1139/111-078>
- [18] Qi J, Wang J, Ma ZJ. Flexural response of high-strength steel-ultra-high-performance fiber reinforced concrete beams based on a mesoscale constitutive model: Experiment and theory. *Struct Concr*. 2018;19:719-34.<https://doi.org/10.1002/suco.201700043>
- [19] Chen S, Zhang R, Jia L-J, Wang J-Y. Flexural behaviour of rebar-reinforced ultra-high-performance concrete beams. *Mag Concr Res*. 2018;70:997-1015.<https://doi.org/10.1680/jmacr.17.00283>
- [20] Lim T, Paramasivam P, Lee S. Shear and moment capacity of reinforced steel-fibre-concrete beams. *Mag Concr Res*. 1987;39:148-60.<https://doi.org/10.1680/macrc.1987.39.140.148>
- [21] Bae B-I, Choi H-K, Choi C-S. Flexural strength evaluation of reinforced concrete members with ultra high performance concrete. *Adv Mater Sci Eng*. 2016;2016. <https://doi.org/10.1155/2016/2815247>
- [22] Khalil WI, Tayfur Y. Flexural strength of fibrous ultra high performance reinforced concrete beams. *ARNP Journal of Engineering and Applied Sciences*. 2013;8:200-14
- [23] Imam M, Vandewalle L, Mortelmans F. Shear–moment analysis of reinforced high strength concrete beams containing steel fibres. *Canadian Journal of Civil Engineering*. 1995;22:462-70. <https://doi.org/10.1139/195-054>.
- [24] Graybeal, B.A. Compression Testing of Ultra-High-Performance Concrete. *Adv. Civ. Eng. Mater.* 2014, 4, 20140027. <https://doi.org/10.1520/acem20140027>.